



Estimation Of Fault Location In Power IEEE 14 Bus System Based On the Value Of Voltage Sag And Phase Angle Using Matching Approach

Lilik Jamilatul Awal¹, Muhammad Akbar Syahbani²,Waldi Abdillah³

^{1,2,3} Universitas Airlangga, Surabaya, 60115, Indonesia

lilik.j.a@ftmm.unair.ac.id

Abstract. The reliability of the electrical network system can be influenced by several factors, one of which is faults. Faults can interrupt the electrical network, leading to severe consequences, including blackouts. The location of the fault needs to be promptly identified to minimize the resulting losses. This research focuses on single-phase-to-ground faults and utilizes voltage sag and phase angle to determine the location of the faults. The method used is the Matching Approach, which identifies the location and distance of fault in the IEEE 14 Bus System. In brief, this method is based on the principle of locating faults through simulation and mathematical approaches. In this study, the data and the implementation of the method are carried out on the transmission network in the IEEE 14 bus power system. Single line-to-ground faults (SLGF) are applied to several nodes, occurring at the n -th second and lasting for half a cycle, causing voltage sag. The estimation of the fault location is simulated using PSCAD software. PSCAD is chosen because it can simulate faults and display real-time results. The research analyzes the fault location for line sections of various lengths: 10 Km, 50 Km, 75 Km, and 100 Km. The results indicate that the Matching Approach method is more accurate when applied to a line length of 10 Km, with an error rate of $<1\%$. The Matching Approach method accurately identifies faulty sections for all line lengths. However, for line lengths of 50 Km, 75 Km, and 100 Km, there is a significant difference between the actual distance and the calculated distance using the Matching Approach method. Thus, estimating the fault location using the Matching Approach method can be implemented in the transmission network, and the maximum applicable section length is 10 Km.

Keywords: Matching Approach, Phase Angle, Transmission System, Voltage Sag

1 Introduction

In an electrical power system, faults are one of the critical factors that impact reliability [1]. Although faults are unavoidable, they can occur due to a range of causes, including malfunctions. [2], [3]. When a fault occurs in the power system, the fault location cannot be determined solely through visual observation[4], [5]. Therefore, a method is needed to determine the location of the fault. There are many methods to locate faults, including the travelling wave and impedance-based methods. These are

first generation methods or classified as conventional methods. These methods identify faults and potential fault locations by comparing the relative distances of each “peak” of the high frequency current signal to a known reflection point in the distribution network [6]. On the other hand, the Impedance-Based method uses impedance values to determine fault location. This method utilizes voltage and current data for impedance calculation [7]. However, implementing these methods still has shortcomings, such as being influenced by system non-homogeneity, measurement errors inline parameters, inaccuracies in relay measurements, and fault resistance[8].

Based on the principle of locating faults in research, detecting fault locations requires a method that is both fast and low in error and economical to reduce operational costs. The Matching Approach method is one such economical method because it only requires measurements at the substation[9]. Thus, this study uses the Matching Approach to identify faults. Moreover, this method can enhance the conventional methods initially developed. It can be implemented in standard networks like the IEEE 14-bus power system analyzed in this study.

The Matching Approach method is applied to identify the location and distance of faults in the power system. Briefly, this method operates by locating faults through simulation and mathematical approaches[10], [11]. When a fault occurs in the power system, observable changes include voltage, current, and phase angle[12]–[14] By utilizing these easily observable variables, voltage, current, and phase angle data are collected through measurements taken at the substation[15]. These variables are compiled into a measurement database. The quick process, ease of use, and high accuracy make this method highly feasible for technicians. Fault location identification using the matching approach has been conducted in [16]–[18], which was applied to distribution networks. This study will be conducted on transmission networks. This contributes to the research by testing different feeder lengths 10 km, 50 km, 75 km, and 100 km.

2. Method

2.1 System Flowchart

Figure 1 represents the overall steps carried out during the research work. The research was conducted on the IEEE 14-bus power system. The system was simulated using PSCAD software. Faults were then simulated at the sending and receiving buses. The simulation data were collected into a measurement database and analyzed mathematically. The next point in the flowchart shows the process of analyzing the faulty section. A section is considered faulty if it satisfies Equations (1) and (2). In this section, the analysis is focused on identifying the part with the highest probability of a fault from the various sections in the network. The research continues with the ranking process. Ranking is performed because more than one section may meet the criteria for a faulty section. The ranking process involves ordering the sections based on the smallest short distance (dk). Once the section with the highest fault probability is identified, the location and distance of the fault can be analyzed using Equation (5).

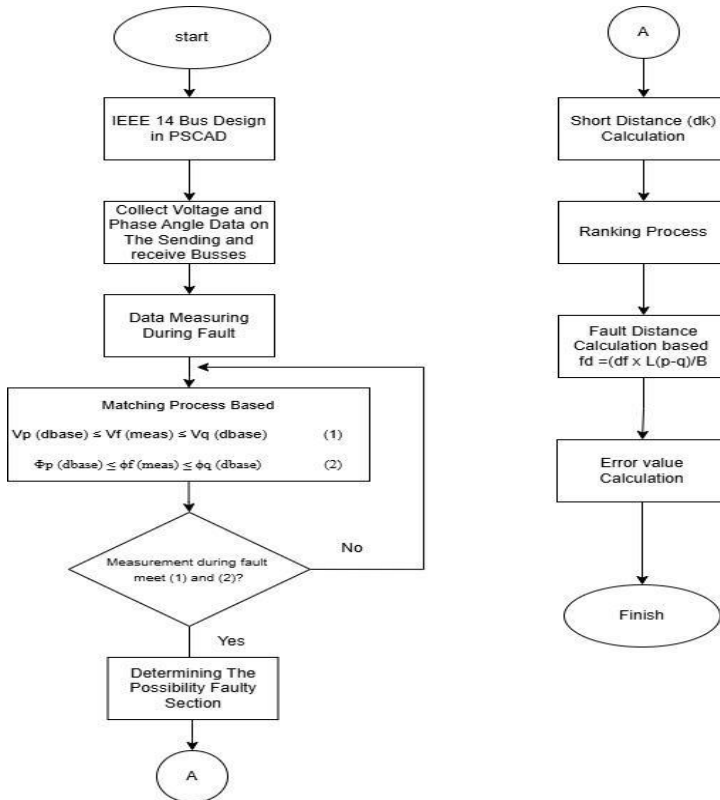


Figure 1. Flowchart of Fault Location

2.2 Testing Power System Network

This research uses data from simulations based on the IEEE 14-bus power system. This circuit model is one of the complex interconnection networks and serves as a standardized network used as a test case for power systems. The IEEE 14-bus system represents the American Electric Power System, consisting of 14 buses, 5 generators, and 11 loads.

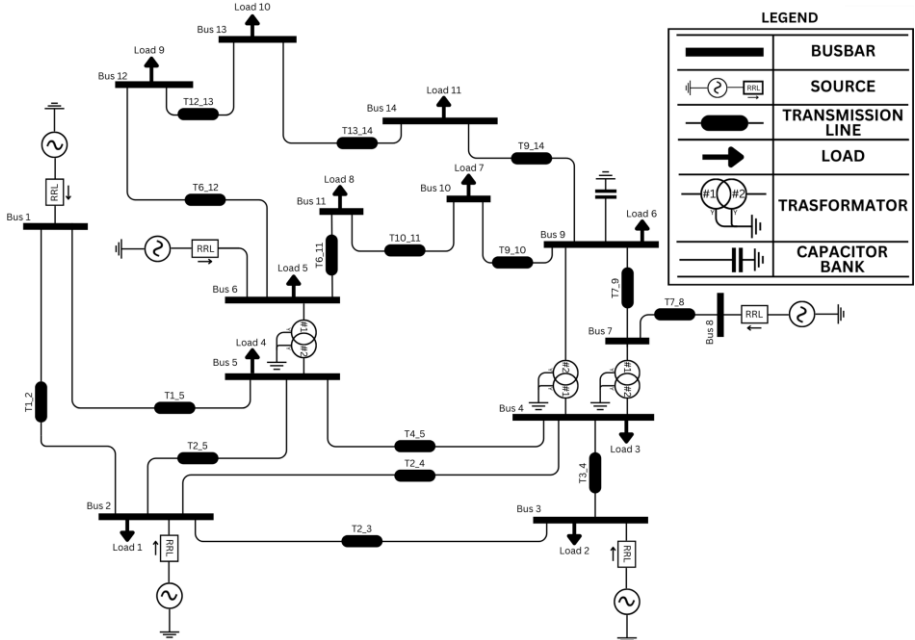


Fig 2. IEEE 14 Bus System Network

Figure 2 depicts the IEEE 14-bus power system created in the PSCAD software. A single phase to ground fault will be applied at one of the locations between adjacent feeders. In this network, the type and timing of the fault can be implemented in real time. From the fault simulation results, voltage sag, current, and phase angle will be obtained and stored in a database.

2.3 Faulty Section Identification

The faulty section is identified by comparing the magnitude of the actual voltage sags and phase angle due to the fault with the magnitude of the voltage sags and phase angle in the database. The section likely experiencing the fault is selected when the magnitude of the voltage sag and phase angle fall between the voltage sag magnitude and phase angle values of two adjacent nodes, as shown in Equations (1) and (2) below [15].

$$V_p \text{ (dbase)} \leq V_f \text{ (meas)} \leq V_q \text{ (dbase)} \tag{1}$$

$$\Phi_p \text{ (dbase)} \leq \phi_f \text{ (meas)} \leq \phi_q \text{ (dbase)} \tag{2}$$

2.4 Fault Distance Analysis

Fault distance is the fault location analysis calculated within the faulty section. In the results of this research, the fault distance will be presented in kilometers. The identified distance is measured from the sending bus. In this fault distance calculation, a mathematical approach is used, as shown in the following equation[18].

$$Fd = \left| \frac{df}{l(p-q)} \right| \times \text{length section} \quad (5)$$

$$df = \sqrt{(V_f - V_p)^2 + (\varphi_F - \varphi_S)^2} \quad (6)$$

$$l(p-q) = \sqrt{(V_q - V_p)^2 + (\varphi_P - \varphi_S)^2} \quad (7)$$

This equation obtains the fault distance using Equation (5), where df represents the assumed distance from the sending bus to the fault point. Meanwhile, L_{p-q} is the actual length of the cable. This equation is based on trigonometric principles. The voltage and phase angle at the sending and receiving buses form coordinates. A linear line is drawn between the coordinates of the sending and receiving buses. The distance between the voltage and phase angle coordinates during the fault simulation is drawn perpendicular to this linear line, allowing Equation (5) to be applied. An illustration of the voltage and phase angle coordinates can be observed in Figure 3.

3. Result

3.1 Fault Distance on Section 10 Km

Based on the analysis of the fault location using Equation (5), the fault distance results obtained using the Matching Approach method are shown in Table 1. This table contains information on the test fault locations in the PSCAD simulation along with the fault distance analysis results using the Matching Approach method. The length of the section used in the test is 10 km. In this 10 km network, the fault is placed in the middle of the network (5 Km). Thus, the accuracy of the Matching Approach method can be assessed. The estimated fault location for the 10 km section shows that the difference between the test fault location in PSCAD and the results from the Matching Approach method is minimal. Therefore, implementing this method for a 10 km IEEE 14-bus transmission network is considered adequate. Table 1 also shows the possible faulty sections and their rankings. This allows the inspection team to repair the network promptly and accurately regarding the fault location.

Table 1. Fault Distance Analysis Section Length 10 Km

<i>Section length</i>	<i>Test Section</i>	<i>Location Test</i>	<i>Fault distance</i>	<i>Possibility Faulty Section</i>	<i>dk</i>	<i>Ranking</i>
10 Km	(9-14)	5 km	5,10 km	(9-14)	0,0148	1
				(9-10)	0,0231	2
				(7-8)	0,05	3
	(2-3)	5 km	4,97 km	(2-3)	0,0342	2
				(3-4)	0,0065	1
	(7-8)	5 km	5,20 km	(7-8)	0,0092	1
	(4-5)	5 km	4,98 km	(4-5)	0,0324	2
				(2-5)	0,0103	1

3.2 Fault Distance on Section 50 Km

The fault location estimation for a section, as shown in Table 2, is analyzed for a 50 km section length. The results indicate that the Matching Approach method can provide accurate fault section results. However, for a 50 km section length, the fault distance estimation using the Matching Approach shows a significant deviation. Additionally, there are several sections ranked 2 and 3. This requires the inspection team to prioritize inspections of the section ranked 1 first, potentially increasing the time needed to repair the network.

Table 2. Fault Distance Analysis Section Length 50 Km

<i>Panjang Section</i>	<i>Test Section</i>	<i>Location Test</i>	<i>Fault distance</i>	<i>Possibility faulty section</i>	<i>dk</i>	<i>Ranking</i>
50 km	(13-14)	25 km	36 km	(13-14)	0,0225	2
				(9-10)	0,006	1
	(10-11)	25 km	36,16 km	(9-10)	0,0194	1
				(10-11)	0,0355	2
				(12-13)	0,0331	3
	(9-10)	25 km	35 km	(9-10)	0,016	1
	(12-13)	25 km	30,62 km	(12-13)	0,0615	1

3.3 Fault Distance on Section 75 Km

The fault location was subsequently estimated by setting the Pi Section component line length in PSCAD to 75 km. The fault was applied in the middle of the line, at 35 km. The deviation from the actual distance at 75 km is quite large. Despite the significant deviation, the faulty section was successfully identified, and the entire system ranked 1. This can be seen in Table 3.

Table 3. Fault Distance Analysis Section Length 75 Km

<i>Panjang</i>	<i>Test Section</i>	<i>Location Test</i>	<i>Fault Distance</i>	<i>Possibility Faulty Section</i>	<i>dk</i>	<i>Ranking</i>
----------------	---------------------	----------------------	-----------------------	-----------------------------------	-----------	----------------

<i>Section</i>						
75 km	(6-13)	35 km	59 km	(6-13)	0,0476	1
				(6-12)	0,0482	2
	(6-12)	35 km	52,05 km	(6-12)	0,0591	1
				(6-13)	0,0597	2
	(2-5)	35 km	63,6 km	(2-5)	0,0508	1
	(6-11)	35 km	50.11 km	(6-12)	0,1326	1

3.4 Fault Distance on Section 100 Km

The fault location estimation using the Matching Approach method was conducted for a section of 100 km. There was a substantial discrepancy between the estimated result and the actual fault location. The most significant deviation occurred at Node 2-4, with the fault positioned at the section’s midpoint (50 km). Although the deviation was considerable, the method successfully identified the faulty section at this distance. The process can indicate where the fault happened for a 100 km section, though the fault distance varies significantly from the actual location.

Table 4. Fault Distance Analysis Section Length 100 Km

<i>Panjang Section</i>	<i>Test Section</i>	<i>Test Lokasi</i>	<i>Fault Distance</i>	<i>Possibility Faulty Section</i>	<i>dk</i>	<i>Ranking</i>
100 km	(1-2)	50 km	35,88 km	(1-2)	0,216	2
				(2-4)	0,0045	1
	(1-5)	50 km	79,148 km	(2-4)	0,0169	2
				(1-5)	0,081	1
				(1-2)	0,2177	3
	(2-4)	50 km	88,9 km	(1-2)	0,1784	1
				(2-4)	0,2326	2
	(3-4)	50 km	85,78 km	(1-2)	0,1831	1
			(3-4)	0,1907	2	

3.5 Error Analysis on Section Length 10 km

Figure 4 illustrates the error values for fault testing with a section length of 10 km. The simulation results showed minimal fault distance discrepancy compared to the fault location analysis using the Matching Approach method. The total network length in this simulation is 160 km. The fault simulation test at this distance had an error of less than 1%. The Matching Approach method remains applicable based on the 10 km section test results.

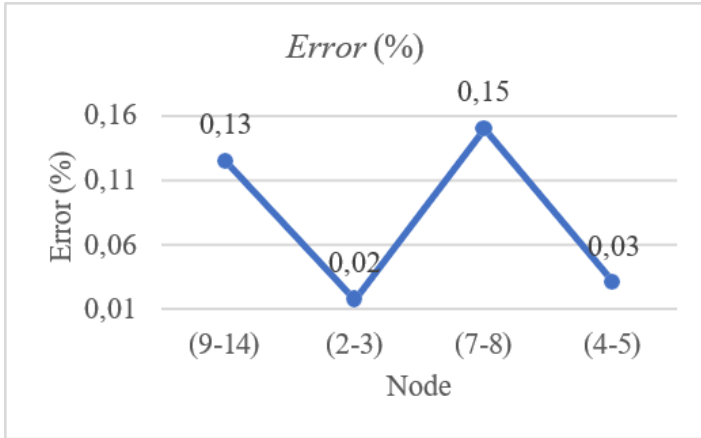


Figure 4. Error Measurement on 10 Km Feeder Length

3.6 Error Analysis on Section Length 50 km

Figure 5 presents a graph that shows the error values during fault testing across different sections. The fault test distance was randomly placed for each section. The results from the Matching Approach method displayed a considerable difference compared to the test distances in PSCAD. Although the Matching Approach successfully pinpointed the section where the fault occurred, the discrepancy between the estimated and actual distances was still quite large. The section length, in this case, was 200 km. For a section length of 50 km, the Matching Approach method yielded an error within a 5% range. Even though there was a significant distance deviation, the error remained within 5%, indicating that the Matching Approach can still be used for a 50 km section, though it is not advisable.

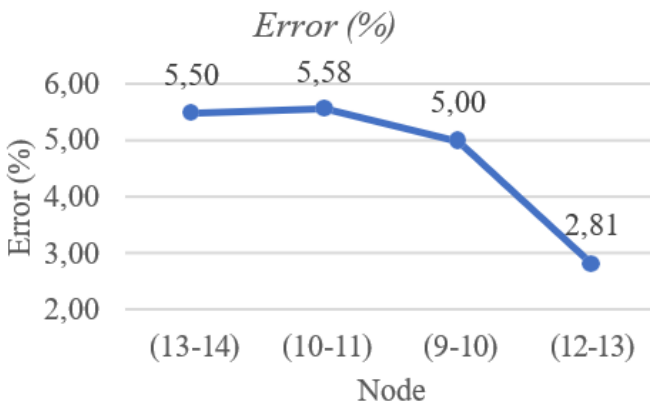


Figure 5. Error Measurement on 50 Km Feeder Length

3.7 Error Analysis on Section Length 75 km

Figure 6 shows a graph illustrating the percentage error in fault location estimation. The total network length is 225 km. In the 75 km section test, faults were tested at random distances, as shown in Figure 6. The results revealed a significant distance discrepancy, with error percentages exceeding 5%. This indicates that the Matching Approach method is not recommended for fault location analysis at this distance.

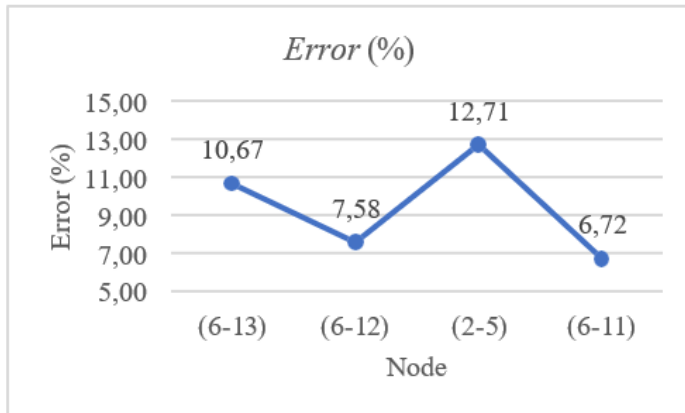


Figure 6. Error Measurement on 75 Km Feeder Length

3.8 Error Analysis on Section Length 100 km

In the fault testing for a 100 km section, there was a significant discrepancy between the actual fault location and the results from the Matching Approach method, as shown in Figure 7. This testing was conducted on a network with a total line length of 250 km. The Matching Approach method produced a distance error with a percentage greater than 5%. Therefore, applying the Matching Approach method for this distance in the IEEE 14-bus transmission system is not recommended.

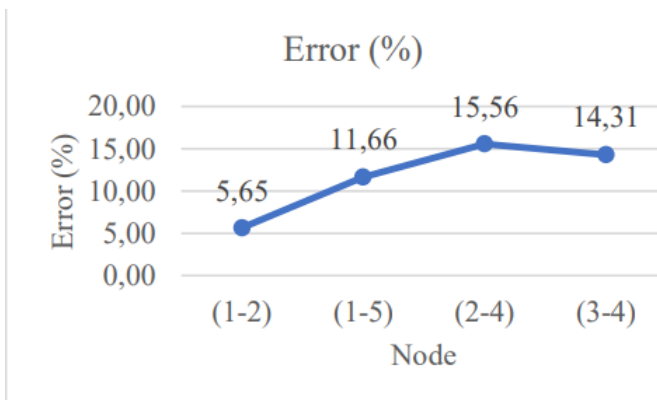


Figure 7. Error Measurement on 100 Km Feeder Length

4. Discussion

4.1 Analysis of The Inaccuracy of The Matching Approach Method

In the fault location analysis using the Matching Approach method, faults were assessed on sections of 10 km, 50 km, 75 km, and 100 km. The variations in section length were tested to determine which section length could accurately analyze fault locations using the Matching Approach. The research results indicated that fault location estimation for sections of 50 km, 75 km, and 100 km was inaccurate due to significant discrepancies between the actual and measured distances.

As proposed by Awalin et al. 2019, the Matching Approach method was initially designed for distribution networks, typically characterized by shorter line lengths. In contrast, this study applied the Matching Approach to long-distance transmission networks. Voltage measurements taken from substations show that the sag voltage at the receiving bus is lower than the sending voltage due to resistance effects. As a result, more extended networks tend to have higher measurement errors. In the IEEE 14-bus transmission system, there are instances where the mistake in longer sections can be more minor compared to shorter distances from the sending bus, influenced by the presence of other power flows.

The entire power flow shifts to the fault point when a fault occurs, as illustrated in Figure 8.

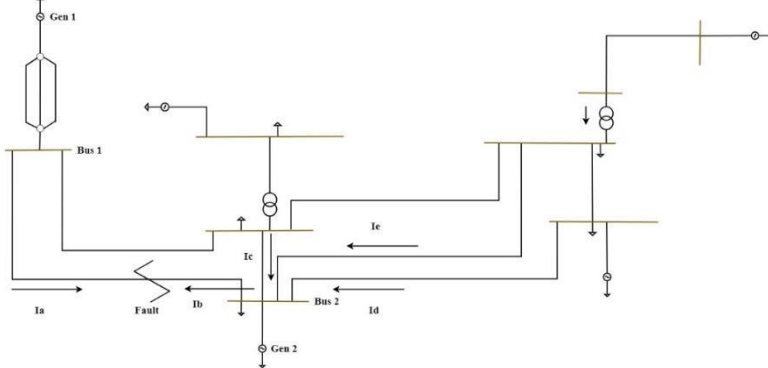


Figure 8 illustrates the condition of buses 1-2. During the fault simulation test for this section, faults were tested at distances of 2 km, 3 km, 4 km, and 7 km within a section length of 10 km and a total network length of 160 km. The error for the 2 km distance was 0.43%, which increased to 0.725% at 3 km and rose to 0.944% at 4 km. However, the error decreased to 0.3% at 7 km. According to Hazlie Mokhlis & Li, 2011, the error at 7 km should have been more significant. Still, in this testing scenario, as shown in Table 5, the error at 7 km is relatively small due to the influence of power flow. Voltage analysis due to contributions from other power sources was calculated as follows.

$$V_a = I_a \times Z_{line\ 7km} + Z_{line\ 3km} \times (I_b + I_c + I_d + I_e) + R_f \times (I_a + I_b + I_c + I_d + I_e) \tag{8}$$

Where I_a , I_b , I_c , I_d , I_e are the currents from the generator shown in Figure 8. Furthermore, R_f is the fault resistance and the Z line is the impedance of the distance to the fault point. The fault occurred 7 km from the first generator, near the second

generator. This proximity allows the second generator to contribute to the power flow during the voltage drop, minimizing the error, as shown in Table 5.

Table 5. Error Fault Distance Analysis

Voltage Sag	Fault Test Distance	Fault Distance Calculation	Error
15, 881	2 Km	1,35 Km	0,47 %
16,347	3 Km	1,85 Km	0,70 %
16,916	4 Km	2,5 Km	0,94%
17, 934	7 Km	6,52 Km	0,3 %

5. Conclusion

Based on the fault location and distance estimation study findings, the following points were observed.

- The Matching Approach method is effective in transmission networks with a maximum viable length of 10 km.
- The method can be applied to transmission networks up to 10 km long.
- The fault distance estimation using the Matching Approach method has an error margin of less than 1% for a test section of 10 km.
- For sections of 50 km, the error rate increases to approximately 5%. While the Matching Approach method can still be applied at this distance, it is not advisable due to the significant deviation.
- For section lengths of 75 km and 100 km, the estimation errors become substantial, exceeding 5%, rendering the Matching Approach method impractical for these distances.

Acknowledgments. The authors thank the Research Center for New and Renewable Energy Engineering, Universitas Airlangga, for providing research facilities. We also thank all colleagues and students of Electrical Engineering from the Faculty of Advance Technology and Multidiscipline, Airlangga University, for supporting this research.

References

- [1] B. Xia, Y. Wang, E. Vazquez, W. Xu, D. Wong, and M. Tong, "Estimation of fault resistance using fault record data," *IEEE Trans. Power Deliv.*, vol. 30, no. 1, pp. 153–160, 2015, doi: 10.1109/TPWRD.2014.2355041.
- [2] A. D. Filomena, M. Resener, R. H. Salim, and A. S. Bretas, "Distribution systems fault analysis considering fault resistance estimation," *Int. J. Electr. Power Energy Syst.*, vol. 33, no. 7, pp. 1326–1335, 2011, doi: 10.1016/j.ijepes.2011.06.010.
- [3] V. De Andrade and E. Sorrentino, "Typical expected values of the fault resistance in power systems," *2010 IEEE/PES Transm. Distrib. Conf. Expo. Lat. Am. T D-LA 2010*, pp. 602–609, 2011, doi: 10.1109/TDC-LA.2010.5762944.
- [4] A. K. Abbas, S. Hamad, and N. A. Hamad, "Single line to ground fault detection and

- location in medium voltage distribution system network based on neural network,” *Indones. J. Electr. Eng. Comput. Sci.*, vol. 23, no. 2, p. 621, 2021, doi: 10.11591/ijeecs.v23.i2.pp621-632.
- [5] H. H. Chang, T. C. Lai, H. J. Chang, and W. J. Lee, “Transmission-Line Fault Location Identifications in H.V. Transmission Networks and different MV Wind Farms using Non-intrusive Monitoring Techniques,” *Conf. Rec. - IAS Annu. Meet. (IEEE Ind. Appl. Soc.)*, vol. 2021-October, no. 2, pp. 1822–1830, 2021, doi: 10.1109/IAS48185.2021.9677419.
- [6] L. J. Awalin, H. Mokhlis, M. K. Rahmat, S. Shilpa, F. Albatsh, and B. Ismail, “Fault distance identification using impedance and matching approaches on distribution network,” *Indones. J. Electr. Eng. Comput. Sci.*, vol. 8, no. 3, pp. 770–778, 2017, doi: 10.11591/ijeecs.v8.i3.pp770-778.
- [7] L. J. Awalin, H. Mokhlis, and A. H. A. Bakar, “Recent developments in fault location methods for distribution networks,” *Prz. Elektrotechniczny*, vol. 88, no. 12 A, pp. 206–212, 2012.
- [8] V. C. Nikolaidis, A. M. Tsimtsios, and A. S. Safigianni, “Investigating particularities of infeed and fault resistance effect on distance relays protecting radial distribution feeders with DG,” *IEEE Access*, vol. 6, pp. 11301–11312, 2018, doi: 10.1109/ACCESS.2018.2804046.
- [9] S. S. Gururajapathy, H. Mokhlis, and H. A. Illias, “Fault location and detection techniques in power distribution systems with distributed generation: A review,” *Renew. Sustain. Energy Rev.*, vol. 74, no. February 2016, pp. 949–958, 2017, doi: 10.1016/j.rser.2017.03.021.
- [10] L. J. Awalin, Tasnim, T. L. Tien, and H. Suyono, “Comparison study of fault location on distribution network using PSCAD and DIGSILENT power factory by using matching approaches,” *Indones. J. Electr. Eng. Comput. Sci.*, vol. 17, no. 1, pp. 78–85, 2019, doi: 10.11591/ijeecs.v17.i1.pp78-85.
- [11] L. Ma, Y. Li, D. Tian, J. Lou, Y. Chen, and X. Liu, “Assessment of voltage sag/swell in the distribution network based on energy index and influence degree function,” *Electr. Power Syst. Res.*, vol. 216, no. December 2022, 2023, doi: 10.1016/j.epsr.2022.109072.
- [12] S. Xie, X. Wang, C. Qu, X. Wang, and J. Guo, “Impacts of different wind speed simulation methods on conditional reliability indices,” *Int. Trans. Electr. energy Syst.*, vol. 20, no. July 2013, pp. 1–6, 2013, doi: 10.1002/etep.
- [13] S. Kaur and N. Kaur, “Application of Optimization Techniques to Mitigate Voltage Sag and Swell by Using Real Time Values,” *Proc. Int. Conf. Electron. Renew. Syst. ICEARS 2022*, no. Icears, pp. 166–173, 2022, doi: 10.1109/ICEARS53579.2022.9751971.
- [14] D. Paul, “Phase-Ground Fault Current Analysis and Protection of a High-Resistance Grounded Power System,” *IEEE Trans. Ind. Appl.*, vol. 56, no. 4, pp. 3306–3314, 2020, doi: 10.1109/TIA.2020.2990116.
- [15] L. J. Awalin, H. Mokhlis, A. Abu Bakar, H. Mohamad, and H. A. Illias, “A generalized fault location method based on voltage sags for distribution network,” *IEEJ Trans. Electr. Electron. Eng.*, vol. 8, no. SUPL.1, 2013, doi: 10.1002/tee.21916.
- [16] H. Mokhlis and H. Y. Li, “Fault location estimation for distribution system using simulated voltage sags data,” *Proc. Univ. Power Eng. Conf.*, no. 1, pp. 242–247, 2007, doi: 10.1109/UPEC.2007.4468953.
- [17] L. J. Awalin, K. Naidu, A. Suyono, and I. Ali, “Automation of faulty type classification considering voltage sag and current swell profile by using MATLAB programming,” *AIP Conf. Proc.*, vol. 2129, no. July, 2019, doi: 10.1063/1.5118142.
- [18] H. Mokhlis and H. Li, “Non-linear representation of voltage sag profiles for fault location in distribution networks,” *Int. J. Electr. Power Energy Syst.*, vol. 33, no. 1, pp. 124–130, 2011, doi: 10.1016/j.ijepes.2010.06.020.
- [19] M. Dashtdar, M. Bajaj, S. M. S. Hosseinimoghadam, and H. Mérshêkáér, “Fault location

in distribution network by solving the optimization problem using genetic algorithm based on the calculating voltage changes.” *Soft Comput.*, vol. 26, no. 17, pp. 8757–8783, 2022, doi: 10.1007/s00500-022-07203-8.

Open Access This chapter is licensed under the terms of the Creative Commons Attribution-NonCommercial 4.0 International License (<http://creativecommons.org/licenses/by-nc/4.0/>), which permits any noncommercial use, sharing, adaptation, distribution and reproduction in any medium or format, as long as you give appropriate credit to the original author(s) and the source, provide a link to the Creative Commons license and indicate if changes were made.

The images or other third party material in this chapter are included in the chapter's Creative Commons license, unless indicated otherwise in a credit line to the material. If material is not included in the chapter's Creative Commons license and your intended use is not permitted by statutory regulation or exceeds the permitted use, you will need to obtain permission directly from the copyright holder.

